

Electron transport in NiCr-O thin films at low temperatures

This article has been downloaded from IOPscience. Please scroll down to see the full text article.

1989 J. Phys.: Condens. Matter 1 10379

(<http://iopscience.iop.org/0953-8984/1/51/011>)

View [the table of contents for this issue](#), or go to the [journal homepage](#) for more

Download details:

IP Address: 129.252.86.83

The article was downloaded on 27/05/2010 at 11:13

Please note that [terms and conditions apply](#).

Electron transport in NiCr–O thin films at low temperatures

H Dintner[†], A Heinrich[‡], C Gladun[‡] and R Mattheis[†]

[†] Akademie der Wissenschaften der DDR, Physikalisch-Technisches Institut, Helmholtzweg 4, Jena 6900, German Democratic Republic

[‡] Akademie der Wissenschaften der DDR, Zentralinstitut für Festkörperphysik und Werkstofforschung, Helmholtzstrasse 20, Dresden 8027, German Democratic Republic

Received 20 February 1989

Abstract. Starting from measurements of the DC conductivity $\sigma(T)$ in the temperature range from 0.05 to 300 K, we can qualitatively describe the electron transport in NiCr–O thin films at low temperatures by its dependence on the atomic oxygen concentration c_O . At a critical value of c_O a metal–insulator transition occurs near $T = 0$. In the metallic region the electrical behaviour can be interpreted in terms of weakly localised electrons including electron correlation. In the non-metallic region an activated temperature dependence is found which is due to variable-range hopping of strongly localised electrons.

1. Introduction

NiCr thin films are widely used as high-performance resistors in microelectronics. In order to achieve the electrical properties required for technical applications, the films are usually vacuum deposited in a reactive atmosphere. In earlier papers dealing with NiCr resistive films (see, e.g., Lassak and Hieber 1973, Polaschegg *et al* 1976, Dintner *et al* 1989) it was found that, when oxygen was the reactive gas, preferential oxidation of chromium takes place during film growth. The resulting heterogeneity of the metallic and non-metallic bonds is essentially restricted to an atomic length scale, i.e. the films can be treated as homogeneous systems (Dintner and Thrum 1989). Because of this, the NiCr–O system belongs to the group of highly disordered materials, e.g. Al–O (Chui *et al* 1981), Al–N (Fortier and Parsons 1987) and CrSi–O (Gladun *et al* 1985) in which as the oxygen or nitrogen concentration increases, the fraction of metallic bonds replaced by non-metallic bonds also increases.

Recently, the dependence of the low-temperature DC conductivity of as-deposited NiCr–O films on the oxygen content has been experimentally investigated in combination with structural studies by means of transmission electron diffraction (Dintner *et al* 1988). It is the aim of this paper to show that the results from films with a metallic conductivity can be properly described within the theoretical framework which has been derived in the past few years for highly disordered metals by taking into account quantum corrections to the semi-classical Boltzmann transport equation (see, e.g., Lee and Ramakrishnan 1985). Moreover, it is argued that the electron transport in highly oxidised NiCr–O thin films exhibiting non-metallic behaviour at low temperatures is due to variable-range hopping of localised electrons (Efros and Shklovskij 1975, Mott and Davis 1979).

The paper is organised as follows. In § 2 some experimental details concerning the preparation and characterisation of the films are given. The results of the low-temperature measurements are presented in § 3 and interpreted with respect to the dominant transport processes in § 4. Finally, some consequences for the resistive films at high temperatures are briefly indicated in § 5.

2. Experimental details

2.1. Film preparation

The NiCr–O films with a mean thickness of about 120 nm were reactively deposited by DC magnetron sputtering of a sintered target ($[\text{Ni}]/[\text{Cr}] = 43/57$, where the concentrations $[\text{Ni}]$ and $[\text{Cr}]$ are in atomic per cent) in an Ar–O₂ atmosphere at various oxygen partial pressures. Thermally oxidised Si wafers (th-SiO₂) and polished plates of vitreous carbon (v-C) were used as substrates for the electrical measurements and the chemical analysis, respectively. During the deposition processes the temperature T_s of the rotating substrates was automatically adjusted to values of 423 K and 573 K, respectively, with an error of less than ± 5 K. The samples used for electrical measurements were patterned by the usual photolithography method.

2.2. Film characterisation

The atomic oxygen concentrations c_O of the films were determined by means of the Rutherford backscattering spectrometry using 1.4 MeV ⁴He particles. Corresponding to the different preparation conditions indicated above, the oxygen contents measured in NiCr–O films on v-C with an error of about 1 at. % varied in the range from about 6 at. % up to more than 40 at. % (for further details see Dintner *et al* (1989)). It has been proved that the results from films which had been simultaneously deposited onto both kinds of substrate were identical within the enlarged error of about ± 3 at. % in the case of the th-SiO₂ substrates.

The measurements of the DC conductivity were performed by the four-probe technique in a refrigerator by which the samples could be cooled to temperatures below 0.1 K. It should be noted that, owing to laterally inhomogeneous incorporation of oxygen, the relationships derived between the experimental values of the conductivity σ and the oxygen concentration c_O could be affected with an additional error of at most 3 at. %.

3. Experimental results

As with increasing oxygen content c_O the NiCr–O films undergo a metal–insulator transition (MIT) at a critical value $c_O = c_O^{\text{MIT}}$ (see below), the presentation of the experimental results follows this separation into a metallic ($c_O < c_O^{\text{MIT}}$) and a non-metallic ($c_O \geq c_O^{\text{MIT}}$) region.

3.1. Metallic region

In figure 1 the temperature dependence of the DC conductivity $\sigma(T)$ normalised to its room-temperature value $\sigma_{300\text{K}}$ is shown for the films deposited at $T_s = 423$ K. The curves

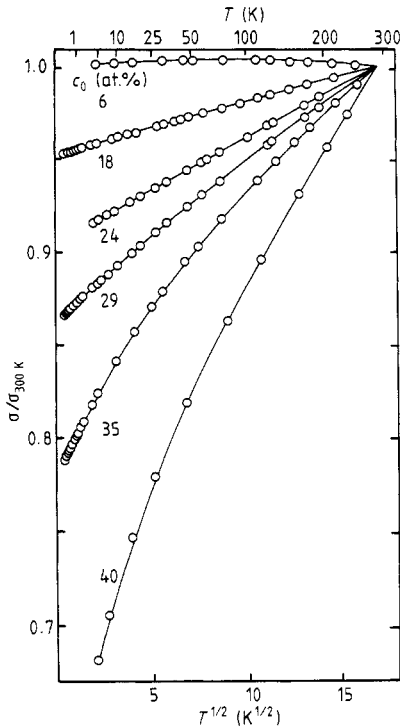


Figure 1. Normalised DC conductivity of NiCr–O films ($[\text{Ni}]/[\text{Cr}] = 43/57$, where $[\text{Ni}]$ and $[\text{Cr}]$ are in atomic per cent); $T_s = 423$ K.

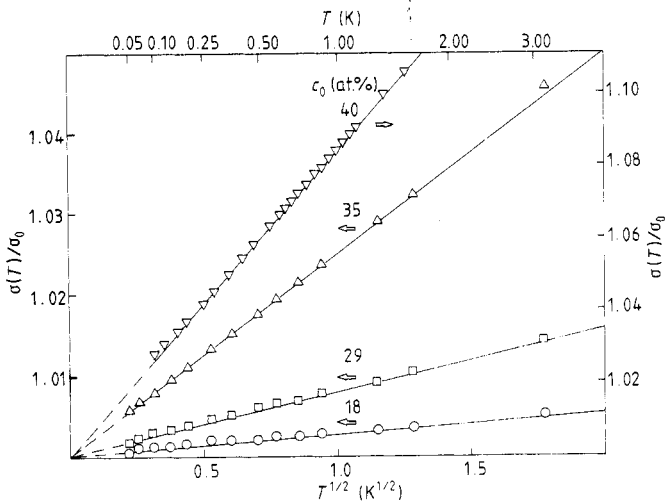


Figure 2. Temperature dependence of the metallic conductivity below 4 K normalized to the extrapolated value at $T = 0$ (same samples as in figure 1).

of all the metallic samples, except the nearly oxygen-free film, can be approximated well by the relation

$$\sigma(T) = \sigma_0 + \alpha T^{1/2} \quad \alpha > 0 \quad T \leq T_{AA} \quad (1)$$

from low temperatures up to an upper limit $T = T_{AA}$. In figure 2 it is demonstrated by an enlarged scale that equation (1) is exactly satisfied in the low-temperature range.

Table 1. Experimental results for metallic NiCr-O films ([Ni]/[Cr] = 43/57, where [Ni] and [Cr] are in atomic per cent) at low temperatures: c_O , atomic oxygen concentration; σ_{300K} , room-temperature conductivity; σ_0 , α and β , fitting parameters of equations (1) and (2), respectively; T_{AA} , upper temperature limit of equation (1).

Sample	T_s (K)	c_O (at. %)	σ_{300K} ($\Omega^{-1} \text{cm}^{-1}$)	σ_0 ($\Omega^{-1} \text{cm}^{-1}$)	α ($\Omega^{-1} \text{cm}^{-1} \text{K}^{-1/2}$)	β ($\Omega^{-1} \text{cm}^{-1} \text{K}^{-1}$)	T_{AA} (K)
1	423	6	7430	7435	7.1	-0.44	—
2	423	18	5270	5021	14.5	-0.23	200
3	423	24	3400	3076	19	-0.18	150
4	423	29	2202	1905	20	-0.17	36
5	423	35	1165	882	22	-0.16	4
6	423	40	609	363	30	-0.11	2
11	573	6	8070	8027	8	-0.53	—
12	573	12	6549	6432	15	-0.44	—
13	573	23	3776	3572	16	-0.26	—
14	573	27	2356	2170	17	-0.24	—
15	573	34	1308	1154	19	-0.19	—
16	573	35	418	241	35	—	0.7

Above T_{AA} the experimental data in figure 1 can be fitted by the superposition in equation (1) of a term linear in T , yielding

$$\sigma(T) = \sigma_0 + \alpha T^{1/2} + \beta T \quad \beta < 0. \quad (2)$$

It should be noted that in this temperature range the fitting parameters α had to be slightly changed in order to obtain an exact approximation. Further, the closer the samples are to the MIT, the poorer is the fit at high temperatures. Near the MIT the films show a $T^{1/2}$ dependence above about 100 K whose slope is smaller than that of the low-temperature behaviour below T_{AA} .

In contrast, the samples prepared at $T_s = 573$ K do not exhibit a pure $T^{1/2}$ dependence, at least at temperatures above 4 K. The only film measured below 4 K (sample 16 with $c_O = 35$ at. %; see table 1) provided a T_{AA} value of 0.7 K. Apart from this single result, all experimental curves can be fitted well by equation (2) in the whole temperature range considered.

In table 1 the fitting parameters obtained for both series of films are given. With increasing oxygen content c_O the values of σ_0 and T_{AA} strongly decrease, whereas the parameters α and β show a marked increase. On the other hand, with rising substrate temperature T_s the conductivity σ_0 only weakly increases. While the parameters α do not alter within the experimental scattering, the parameters β significantly shift to more negative values.

3.2. Non-metallic region

Because from the experimental view the MIT near $T = 0$ is defined by the change in $\sigma(T)$ from a power-law to an exponential dependence, the conductivity $\sigma(T)$ of the non-metallic films is shown in figures 3 and 4 as a plot of $\log \sigma$ against $T^{-\nu}$ with $\nu = \frac{1}{2}$ and $\nu = \frac{1}{4}$, respectively, in order to prove the validity of the relation

$$\sigma(T) = \sigma_{\infty} \exp[-(T_0/T)^{\nu}] \quad (3)$$

($T_0 \equiv T_{ES}$ for $\nu = \frac{1}{2}$; $T_0 \equiv T_M$ for $\nu = \frac{1}{4}$).

For comparison, the $\sigma(T)$ curves of some metallic samples are replotted in figure 3.

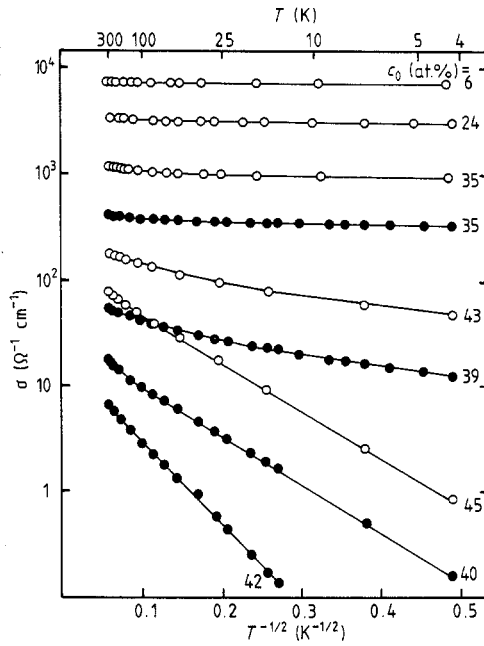


Figure 3. DC conductivity of NiCr-O films ($[\text{Ni}]/[\text{Cr}] = 43/57$, where $[\text{Ni}]$ and $[\text{Cr}]$ are in atomic per cent): \circ , $T_S = 423$ K; \bullet , $T_S = 573$ K.

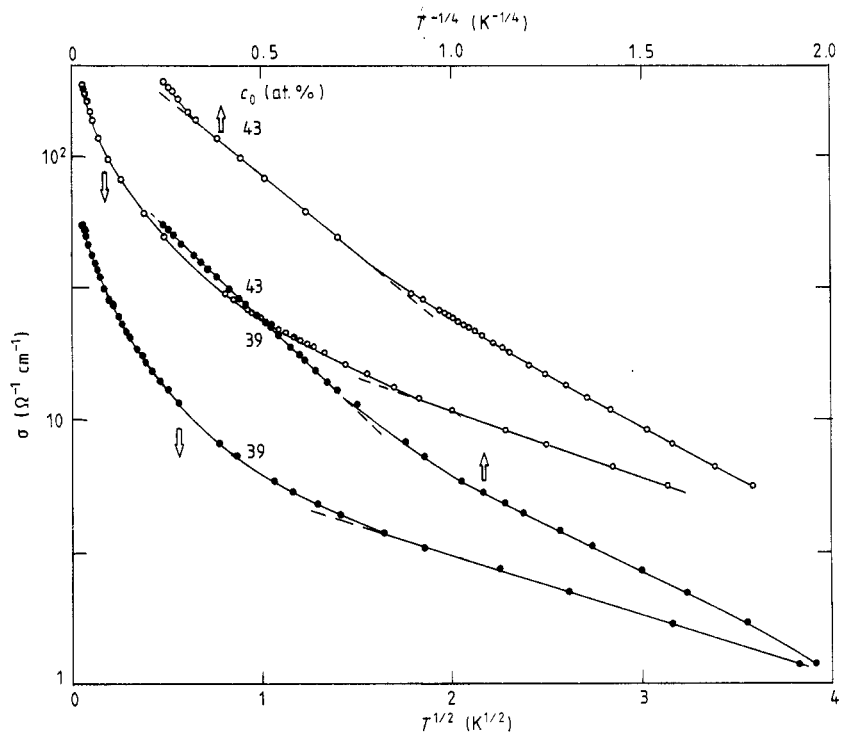


Figure 4. DC conductivity of non-metallic NiCr-O films close to the MIT on a $\log \sigma$ against $T^{-\nu}$ plot with $\nu = \frac{1}{2}$ and $\nu = \frac{1}{4}$ (same samples as in figure 3).

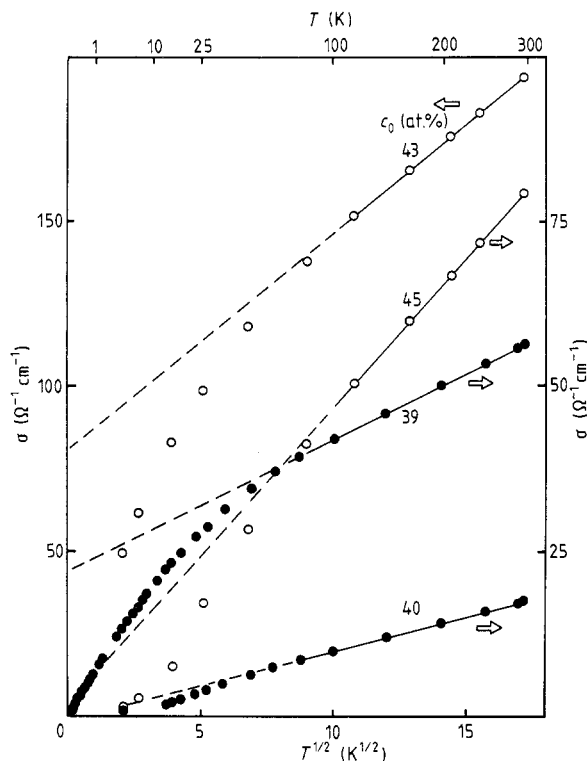


Figure 5. DC conductivity of non-metallic NiCr–O films in a plot showing the non-activated behaviour above 100 K (same samples as in figure 3).

As can be seen, all non-metallic films are described well by equation (3) in the low-temperature region. Depending on the oxygen concentration in the films, far from the MIT only the exponent $\nu = \frac{1}{2}$ is observed up to about $T = T_{ES}$ (figure 3), but in the vicinity of the MIT both exponents are found for $\sigma(T)$: $\nu = \frac{1}{2}$ within the temperature range $0 < T < T_{ES}$ and $\nu = \frac{1}{4}$ within $T_{ES} < T < T_M$ (see figure 4).

In table 2 the fitting parameters T_{ES} , T_M and σ_∞ (corresponding to $\nu = \frac{1}{2}$) are summarised. From this, the temperature T_{ES} strongly rises with increasing oxygen content c_O . The parameters σ_∞ seem to show a non-monotonic behaviour in their dependence on c_O . The rise in the deposition temperature T_S causes a decrease in σ_∞ by about half an order of magnitude at comparable values of T_{ES} . Above the temperature regions

Table 2. Experimental results for non-metallic NiCr–O films ($[\text{Ni}]/[\text{Cr}] = 43/57$, where $[\text{Ni}]$ and $[\text{Cr}]$ are in atomic per cent) at low temperatures: c_O , atomic oxygen concentration; $\sigma_{300\text{K}}$, room-temperature conductivity; σ_∞ , T_{ES} and T_M , fitting parameters of equation (3).

Sample	T_S (K)	c_O (at.%)	$\sigma_{300\text{K}}$ ($\Omega^{-1}\text{cm}^{-1}$)	σ_∞ ($\Omega^{-1}\text{cm}^{-1}$)	T_{ES} (K)	T_M (K)
7	423	43	194	35	0.7	54
8	423	45	79	130	106	—
17	573	39	56	9	0.6	91
18	573	40	17	28	113	—
19	573	42	7	17	325	—

where equation (3) is valid, the conductivity of the films near the MIT changes to a $T^{1/2}$ dependence similar to the metallic samples with $c_O < c_O^{MIT}$ (figure 5). The slope of this dependence is strongly affected by the deposition temperature T_S of the films.

4. Discussion

4.1. Metallic region

Now an attempt is made to discuss the low-temperature conductivity in terms of electron transport in highly disordered metals. In order to provide a starting point, some main theoretical results are cited briefly without an elaborate presentation. If we write the conductivity as $\sigma(T) = \sigma_0 + \sigma_T$, where σ_0 denotes the conductivity at $T = 0$, consideration of the localisation effects yields (cf Abrahams *et al* 1979, Kaveh and Mott 1982)

$$\sigma_0 = \kappa(\frac{1}{3}k_F^2 l_e - 1/l_e) \quad \kappa = e^2/\pi^2 \hbar \quad (4)$$

$$\sigma_T(\text{loc}) = \kappa(1/L_i - k_F^2 l_e^2/l_i) \quad (5)$$

where l_e and l_i are the elastic and inelastic mean free paths, respectively, k_F is the Fermi wavenumber and $L_i = (l_e l_i/3)^{1/2}$ is the diffusion length of the electrons. The contribution of electron-electron interactions first studied by Altshuler and Aronov (1979) can be

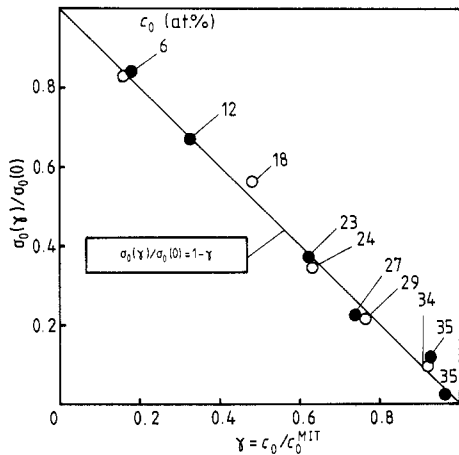


Figure 6. Reduced representation of the dependence of the conductivity at $T = 0$ on the atomic oxygen concentration in the metallic region (linear regression: see text): \circ , $T_S = 423$ K; \bullet , $T_S = 573$ K.

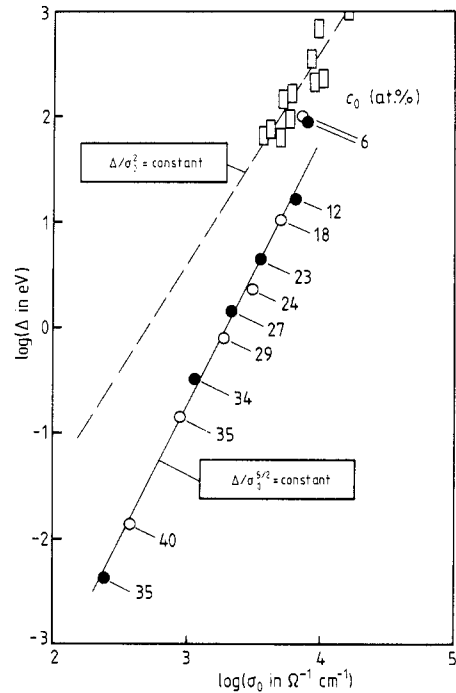


Figure 7. \log - \log plot of the pseudo-gap Δ against the conductivity σ_0 at $T = 0$: \circ , $T_S = 423$ K; \bullet , $T_S = 573$ K; \square , data of Cochrane and Strom-Olsen (1984); ---, taken from Hertel *et al* (1983).

expressed in the notation of Kaveh and Mott (1982) by

$$\sigma_T(\text{int}) = \kappa f(x)(k_B T/\hbar D)^{1/2} \quad x = (2k_F \lambda)^2 \quad (6)$$

where k_B , D and λ are Boltzmann's constant, the diffusion coefficient of the electrons at the Fermi energy and the screening length of the interaction, respectively. The function $f(x) = 1 - (3/2x) \ln(1+x)$ determines the sign of $\sigma_T(\text{int})$ in its dependence on the electron density. For $k_F l_e \gg 1$, i.e. far from the MIT, it is expected that $f(x) = 1$ (Kaveh and Mott 1982). Whereas equation (6) yields a $T^{1/2}$ dependence of $\sigma(T)$, the positive contributions due to localisation (first term in equation (5)) can result in either a dependence linear in T (electron–electron and/or electron–phonon scattering below the Debye temperature) or a $T^{1/2}$ dependence (electron–phonon scattering near and above the Debye temperature). Additionally, the negative Boltzmann term due to the usual electron–phonon scattering (second term in equation (5)) has to be considered. From this, a universal dependence of $\sigma(T)$ was predicted (see, e.g., Kaveh and Mott 1982, Howson 1984) which has been experimentally found, at least partially, for several disordered metal systems (Thomas *et al* 1982, Howson and Greig 1984, 1986, Fortier and Parsons 1987).

Returning to the experimental results for NiCr–O films, we shall first discuss the conductivity at $T = 0$. For both series the dependence of σ_0 on the oxygen content can be described well by a linear function (figure 6). Introducing the variable γ by $\gamma = c_O/c_O^{\text{MIT}}$, where c_O^{MIT} is the critical atomic oxygen concentration at the MIT defined by $\sigma_0(c_O \geq c_O^{\text{MIT}}) = 0$, the linear regression of the experimental data yields $\sigma_0(\gamma = 0) = 8953 \text{ mho cm}^{-1}$ and $c_O^{\text{MIT}} = 37.8 \text{ at.}\%$ for the films deposited at $T_S = 423 \text{ K}$, but $\sigma_0(\gamma = 0) = 9620 \text{ mho cm}^{-1}$ and $c_O^{\text{MIT}} = 36.8 \text{ at.}\%$ for the samples prepared at $T_S = 573 \text{ K}$. The spread of the experimental points in figure 6 around the resulting straight line

$$\sigma_0(\gamma) = \sigma_0(0)(1 - \gamma) \quad 0 \leq \gamma \leq 1 \quad (7)$$

is mainly caused by the inhomogeneous oxygen distribution across the wafer as is pointed out in § 2.

Regarding the temperature dependence of the conductivity, it can be supposed from equation (5) that the negative sign of the linear term in equation (2) represents the predominant effect of the Boltzmann term compared with the inelastic scattering processes in the presence of localisation. Then the observed positive shift of the parameter β with increasing oxygen concentration c_O and falling deposition temperature T_S would reflect an increase in the contribution due to localisation effects, as expected for more disordered metals. However, it must be noted that this interpretation, if actually correct, is limited to medium and high temperatures where the linear Boltzmann term holds. Thus, at present the physical origin of negative parameters β in the low-temperature region near $T = 0$ is still an open question.

With respect to the observed $T^{1/2}$ dependence, a distinction has to be made. In the films close to the MIT which show a pure $T^{1/2}$ dependence above about 100 K up to 300 K (the upper limit of measurements), obviously, the localisation effects are strong enough to determine the temperature dependence of the conductivity in this range (cf Kaveh and Mott 1982, Howson 1984). However, with regard to the low-temperature $T^{1/2}$ term in equations (1) and (2), as shown in figure 2 by way of example, it follows from the theoretical considerations that this dependence must be attributed to electron correlation according to equation (6). Hence, because of the constancy of the parameter α up to the temperature limit T_{AA} given in table 1, this conclusion can be extended, at least, to the whole temperature range where equation (1) holds. It should be emphasised

that, to our knowledge, the dominance of electron–electron interaction in such a wide temperature region is found experimentally for the first time. The theoretical consequences of this result will be checked with numerical estimations below.

On the basis of this interpretation, equation (1) can be rewritten (Cochrane and Strom-Olsen 1984, Rathnayaka *et al* 1986) in the form

$$\sigma(T) = \sigma_0[1 + (k_B T/\Delta)^{1/2}] \quad (8)$$

where Δ is the width of the pseudo-gap in the density of states around the Fermi energy. According to an empirical rule (Hertel *et al* 1983, Cochrane and Strom-Olsen 1984) the relation $\Delta/\sigma_0^2 = \text{constant}$ should be generally valid for disordered metals. However, as shown in figure 7 together with the data of Cochrane and Strom-Olsen (1984), the relation $\Delta/\sigma_0^{2.5} = \text{constant}$ is found in the case of NiCr–O films disregarding both the samples with the lowest oxygen content. Note the difference in the systems studied. Instead of a pure metallic system the NiCr–O films contain a certain amount of non-metallic bonds due to the oxygen incorporation. In this sense it is quite consistent that the nearly oxygen-free samples agree with the data taken from the literature, i.e. these films still show the behaviour of pure metals. From figure 7 a relation for the parameter α as a function of the normalised oxygen concentration γ can be derived, yielding by use of equation (7)

$$\alpha(\gamma) = u/(v + 1 - \gamma)^{1/4} \quad (9)$$

where u and v are constants. (The constant $v (\ll 1)$ has been introduced in order to avoid a singularity of α at the MIT.)

Now, the relations concerning σ_0 (equations (4) and (7)) as well as those describing the parameter α (equations (6) and (9)) can be combined with each other. Using the free-electron approximation the diffusion coefficient D of the Fermi electrons equals $\hbar k_F l_e / 3m$, where m denotes the effective electron mass. Under the assumptions that, firstly, the effective electron mass does not depend on the oxygen concentration and, secondly, the function $f(x)$ in equation (6) is constant in the metallic region sufficiently far from the MIT, i.e. $f(x) = 1$ for $\gamma < 1$ (see above), the Fermi wavenumber k_F and the elastic mean free path l_e are given by

$$k_F(\gamma) = [3^{1/2} \sigma_0(0) / \kappa C] [C(1 - \gamma) + 1]^{1/2} \quad (10)$$

$$l_e(\gamma) = \kappa C / \sigma_0(0) = \text{constant} \quad (11)$$

where the constant C_{H} is defined by

$$C = 3[\kappa(k_B m)^{1/2} f(x) / \hbar \alpha(0)]^4 - 1. \quad (12)$$

As demanded by the Ioffe–Regel criterion (see, e.g., Mott 1987), the MIT at $\gamma = 1$ is included in equations (10) and (11) by the condition $k_F^2 l_e^2 = 3$. Because the Fermi wavenumber is directly related to the density of charge carriers, hence equation (10) reflects the transition of Fermi electrons to lower (bound) states due to the increasing formation of non-metallic Cr–O bonds. On the other hand, regarding equation (11) the degree of disorder characterised by the elastic mean free path (Tsuei 1986) does not depend on the oxygen concentration. This result qualitatively confirms structural studies on NiCr–O films (Dintner *et al* 1988) which did not provide any hint at a more disordered (amorphous) state of the atomic short-range order in the course of oxygen incorporation. Consequently, the NiCr–O films must be rather considered in an analogous way to highly doped semiconductors where, indeed, a dependence of the parameter α on the carrier

density has generally been found (cf Altshuler and Aronov (1985) and references therein).

In order to obtain more quantitative insight, some numerical estimations are given by way of example. If we start from an assumed Fermi wavenumber $k_F(0)$ for oxygen-free films of $1.2 \times 10^8 \text{ cm}^{-1}$, which corresponds to a carrier density of about $6 \times 10^{22} \text{ cm}^{-3}$ in the free-electron theory, the elastic mean free paths l_e are $7.8 \times 10^{-8} \text{ cm}$ and $8.4 \times 10^{-8} \text{ cm}$ for the films prepared at $T_S = 423 \text{ K}$ and $T_S = 573 \text{ K}$, respectively. Furthermore, using $\alpha(0) = 12 \Omega^{-1} \text{ cm}^{-1} \text{ K}^{-1/2}$, as extrapolated from the experimental data by equation (9), the effective electron mass can be estimated to about $7m_0$, where m_0 is the free-electron mass. Hence, both quantities, l_e and m , are obtained with a physically reasonable order of magnitude (Tsuei 1986, Ashcroft and Mermin 1979).

With regard to the experimental observation of electron correlation in the temperature range $T \leq T_{AA}$ it has to be considered that the existence of electron–electron interaction is restricted by the conditions $k_B T < \Delta$ and $k_B T < \hbar \tau_e^{-1}$ (Altshuler and Aronov 1979). Here τ_e denotes the elastic relaxation time given in the free-electron approximation by $\tau_e = l_e m / \hbar k_F$. As the values estimated above yield $\tau_e < 10^{-14} \text{ s}$, the dominance of electron correlation can be expected up to temperatures of some 10^2 K . Moreover, together with figure 7, the increase in τ_e with higher oxygen concentrations c_O provides a possible explanation of the observed $T_{AA}(c_O)$ dependence.

4.2. Non-metallic region

There are two different approaches to the derivation of an exponential temperature dependence of the conductivity as given by equation (3):

(i) variable-range hopping between localised states with a constant density of states around the Fermi energy ($\nu = \frac{1}{4}$ (Mott 1968, Mott and Davis 1979)) or with a Coulomb gap at E_F due to electron correlation ($\nu = \frac{1}{2}$ (Efros and Shklovskij 1975, Efros 1976)). The origin of the localised states can be either atomic defects (as dopants in crystalline or amorphous semiconductors) or metal clusters, e.g. grains as realised in granular metals (Entin-Wohlman *et al* 1983, Nemeth and Mühlischlegel 1988);

(ii) tunnelling of thermally activated charge carriers from charged grains to neutral grains assuming a heterogeneous structure of the system considered, as in granular metals and cermets below the percolation threshold (Abeles *et al* 1975, Sheng and Klafter 1983).

Independent of the origin of the localised states, in the case of variable-range hopping of interacting electrons a change from $\nu = \frac{1}{2}$ at low temperatures to Mott's $\nu = \frac{1}{4}$ takes place with rising temperature owing to the increase in the hopping energies and the growing importance of electron states outside the Coulomb gap. Even such a transition of the exponent ν was experimentally observed (see figure 4).

On the other hand, tunnelling transport from charged to neutral grains in granular metals would just yield the reverse sequence of the exponent ν with temperature (Sheng and Klafter 1983). Therefore, it can be concluded that variable-range hopping is the relevant transport mechanism in the non-metallic NiCr–O films.

The dependence of the parameters T_{ES} and σ_∞ on both the oxygen concentration c_O and the deposition temperature T_S , as given in table 2, can be qualitatively discussed in a manner analogous to the interpretation of the low-temperature behaviour of semi-conducting CrSi and CrSi–O films (Gladun *et al* 1985, Möbius *et al* 1985). From this, the rise in T_{ES} at a constant value of σ_∞ with increasing c_O means that the distance between

the localisation centres increases in relation to the localisation length without a change in the localised states. On the other hand, the observed decrease in σ_x with rising T_S implies a change in the centres (e.g. growth of metal clusters).

Although, to our knowledge, there have up to now been no detailed structural studies on highly oxidised NiCr–O films concerning the size of possible metal clusters, the small values of T_M given in table 2 may be estimated as a hint against a cermet-like structure (Nemeth and Mühlischlegel 1988).

In addition, the transition from equation (3) to a power law, as found in films near the MIT with increasing temperature (see figure 5), can be attributed to the decrease in the (temperature-dependent) hopping length below the localisation length (Larkin and Khmel'nitskij 1982) resulting in a $T^{1/2}$ behaviour owing to the dominance of electron–phonon scattering in the presence of localisation. Hence, this result provides a further hint at a homogeneous structure of the NiCr–O films in the non-metallic region.

5. Conclusions

In summary, from the measurements of the DC conductivity a comprehensive physical interpretation of the electron transport in NiCr–O films at low temperatures has been derived. In particular, it was shown that in the metallic region the $\sigma(T)$ curves can be described in terms of weakly localised electrons including electron–electron interaction.

As the composition and preparation conditions of the metallic films under consideration are identical with those of NiCr–O resistive films used in microelectronics, the conclusions concerning the dominant processes and structural consequences are important not only from a physical point of view but also with regard to practical purposes. Above all, the decrease in the Fermi wavenumber (carrier density) and the constancy of the elastic mean free path (degree of disorder) with increasing oxygen incorporation, which have been derived from the low-temperature measurements, are in agreement with structural studies and provide a useful guide to a deeper understanding of the electrical behaviour in the temperature range relevant for technical applications. These conclusions will be considered in more detail in a forthcoming paper.

Acknowledgments

The authors would like to thank Dr H Bartuch for preparing the NiCr–O films and Dr H Vinzelberg for helping with the low-temperature measurements. With regard to the determination of the oxygen concentrations by Rutherford backscattering spectroscopy the kind support by the colleagues of the Friedrich Schiller University of Jena (Department of Physics) is gratefully acknowledged.

References

- Abeles B, Sheng P, Coutts M D and Arie Y 1975 *Adv. Phys.* **24** 407
- Abrahams E, Anderson P W, Licciardello D C and Ramakrishnan T V 1979 *Phys. Rev. Lett.* **42** 673
- Altshuler B L and Aronov A G 1979 *Zh. Eksp. Teor. Fiz.* **77** 2028
- 1985 *Modern Problems in Condensed Matter Science* ed. A L Efros and M Pollak (Amsterdam: North Holland)
- Ashcroft N W and Mermin N D 1979 *Solid State Physics* vol I (Moscow: Mir)

- Chui T, Deutscher G, Lindenfeld P and McLéan W L 1981 *Phys. Rev. B* **23** 6172
- Cochrane R W and Strom-Olsen J O 1984 *Phys. Rev. B* **29** 1088
- Dintner H, Bartuch H, Heinrich A, Thrum F, Gladun C and Holzhüter G 1988 *Thin Solid Films* **164** 455
- Dintner H, Mattheis R and Vogler G 1989 *Thin Solid Films* **181** at press
- Dintner H and Thrum F 1989 *Phys. Status Solidi a* **111** 551
- Efros A L 1976 *J. Phys. C: Solid State Phys.* **9** 2021
- Efros A L and Shklovskij B I 1975 *J. Phys. C: Solid State Phys.* **8** L49
- Entin-Wohlman E, Gefen Y and Shapira Y 1983 *J. Phys. C: Solid State Phys.* **16** 1161
- Fortier N and Parsons R R 1987 *J. Phys. C: Solid State Phys.* **20** 565
- Gladun C, Heinrich A, Lange F, Schumann J and Vinzelberg H 1985 *Thin Solid Films* **125** 101
- Hertel G, Bishop D J, Spencer E G, Rowell J M and Dynes R C 1983 *Phys. Rev. Lett.* **50** 743
- Howson M A 1984 *J. Phys. F: Met. Phys.* **14** L25
- Howson M A and Greig D 1984 *Phys. Rev. B* **30** 4805
- 1986 *J. Phys. F: Met. Phys.* **16** 989
- Kaveh M and Mott N F 1982 *J. Phys. C: Solid State Phys.* **15** L707
- Larkin A I and Khmel'nitskij D E 1982 *Zh. Eksp. Teor. Fiz.* **83** 1140
- Lassak L and Hieber K 1973 *Thin Solid Films* **17** 105
- Lee P A and Ramakrishnan T V 1985 *Rev. Mod. Phys.* **57** 287
- Möbius A, Vinzelberg H, Gladun C, Heinrich A, Elefant D, Schumann J and Zies G 1985 *J. Phys. C: Solid State Phys.* **18** 3337
- Mott N F 1968 *J. Non-Cryst. Solids* **1** 1
- 1987 *Phys. Status Solidi b* **144** 157
- Mott N F and Davis E A 1979 *Electronic Properties of Non-Crystalline Materials* (Oxford: OUP)
- Nemeth R and Mühlischlegel B 1988 *Z. Phys.* **B 70** 159
- Polaschegg H D, Heinz B and Sommerkamp P 1976 *Vakuum-Technik* **25** 12
- Rathnayaka K D D, Trodahl H J and Kaiser A B 1986 *Solid State Commun.* **57** 207
- Thomas G A, Kawabata A, Ootuka Y, Katsumoto S, Kobayashi S and Sasaki W 1982 *Phys. Rev. B* **26** 2113
- Sheng Ping and Klafter J 1983 *Phys. Rev. B* **27** 2583
- Tsuei C C 1986 *Phys. Rev. Lett.* **57** 1943